Nucleon momentum distribution in deuteron and other nuclei within the light-front dynamics method

A.N. Antonov, M.K. Gaidarov, M.V. Ivanov, and D.N. Kadrev

Institute of Nuclear Research and Nuclear Energy, Bulgarian Academy of Sciences, Sofia 1784, Bulgaria

G.Z. Krumova

University of Rousse, Rousse 7000, Bulgaria

P.E. Hodgson

Subdepartment of Nuclear and Particle Physics, University of Oxford, Oxford OX1-3RH, U.K.

H.V. von Geramb

Theoretische Kernphysik, Universität Hamburg, Hamburg D-22761, Germany

arXiv:nucl-th/0106044v2 9 Nov 2001

The relativistic light-front dynamics (LFD) method has been shown to give a correct description of the most recent data for the deuteron monopole and quadrupole charge form factors obtained at the Jefferson Laboratory for elastic electron-deuteron scattering for six values of the squared momentum transfer between 0.66 and 1.7 (GeV/c)^2. The good agreement with the data is in contrast with the results of the existing non-relativistic approaches.

In this work we firstly make a complementary test of the LFD applying it to calculate another important characteristic, the nucleon momentum distribution $n(q)$ of the deuteron using six invariant functions f_i ($i = 1, ..., 6$) instead of two (S- and D-waves) in the nonrelativistic case. The comparison with the y-scaling data shows the decisive role of the function f_5 which at $q \geq 500$ MeV/c exceeds all other f-functions (as well as the S- and D-waves) for the correct description of $n(q)$ of the deuteron in the high-momentum region. Comparison with other calculations using S- and D-waves corresponding to various nucleon-nucleon potentials is made. Secondly, using clear indications that the high-momentum components of $n(q)$ in heavier nuclei are related to those in the deuteron, we develop an approach within the natural orbital representation to calculate $n(q)$ in (A, Z)-nuclei on the basis of the deuteron momentum distribution. As examples, $n(q)$ in ^{4}He, ^{12}C and ^{56}Fe are calculated and good agreement with the y-scaling data is obtained.

I. INTRODUCTION

The most recent experimental data on the deuteron structure functions and tensor polarizations obtained at Thomas Jefferson Laboratory have been reported in [1–6] (and references therein). The new data on tensor polarization observables measured in elastic electron-deuteron scattering for the squared momentum transfer between 0.66 and 1.7 (GeV/c)^2 [1] make it possible to determine quite precisely the deuteron charge form factors for momenta comparable with the deuteron mass. Thus these data are important to probe the relativistic dynamics inside the deuteron. It was shown in [1] that the empirical results for the tensor polarization t_{20} and both monopole (G_C) and quadrupole (G_Q) charge form factors are in very good agreement with the calculations within two relativistic and covariant models: i) a model developed in the framework of the explicitly covariant version of light-front dynamics (LFD) (e.g. [7–10]) and, ii) a model using a three-dimensional reduction of the Bethe-Salpeter equation [11]. At the same time the non-relativistic impulse approximation approach [12] (even with inclusion of meson exchange currents and relativistic corrections) cannot explain, for instance, the behaviour of the monopole charge form factor in the region of the first node and the secondary maximum shown for the first time in [1].

It is well known [13–15] that one of the main feature of the realistic nuclear models (beyond the mean-field approximation) is that they have to describe *simultaneously* both important ground state characteristics, the nucleon momentum and density distributions of the system. This is not the case in the Hartree-Fock approximation where the dynamical short-range and tensor nucleon-nucleon (NN) correlations are only partly incorporated. The main characteristic feature of the data on the nucleon momentum distribution $n(q)$ extracted by the nuclear y-scaling analysis [16–19] (we shall call them all along this paper y-scaling data (YSD)) is the existence of high-momentum components for momenta $q > 2$ fm^{-1} due to the short-range and tensor NN correlations. This has been shown also for particular nuclei such as ^{2}H, ^{3,4}He, ^{12}C, ^{16}O, ^{40}Ca and others and in nuclear matter within various theoretical correlation methods (see e.g. [20–40] and reviews in [14,15]). In addition, both experimental and theoretical analyses confirm the conclusion that the high-momentum behaviour of the nucleon momentum distribution ($n(q)$/A at $q > 2$ fm^{-1}) is similar for nuclei with mass numbers A=2, 3, 4, 12 and 56 and for nuclear matter.

The first aim of the present work is to apply the LFD method to calculations of the momentum distribution in the deuteron. Thus this study is an *important complementary test* of the possibility of the LFD *to describe simultaneously* both deuteron charge form factors (that has been shown in [1]) and momentum distribution. In this line the results of calculations using wave functions of existing NN potentials are also given and compared with the LFD results and the YSD.

The second aim of the work is to develop a method which would allow us to calculate the nucleon momentum distribution for a wide range of (A, Z)-nuclei on the basis of the knowledge of $n(q)$ in the deuteron and especially of its high-momentum components. The latter are important because in various processes with high transferred momenta only relativistic nucleons can take part [8]. Such analyses require the knowledge of the wave function (WF) at momenta with magnitude of the nucleon mass. We make an attempt to relate the relativistic effects in $n(q)$ in the deuteron with the explanation of the high-momentum components of $n(q)$ in heavier nuclei which are important for calculations of the cross sections of various nuclear reactions. This question is discussed together with the effects of short-range NN correlations on the nucleon momentum distributions.

A brief review of the LFD method is given in Sect. II. The results of the calculations of $n(q)$ in deuteron within the LFD and the comparison with calculations using wave functions corresponding to existing NN potentials and the YSD are given in the same Section. In Sect. III a method to calculate the nucleon momentum distribution in (A, Z)-nuclei is developed using the natural orbital representation and the results on the high-momentum components of the nucleon momentum distribution in the deuteron. Sect. IV contains the conclusions of the present work.

II. NUCLEON MOMENTUM DISTRIBUTION IN THE DEUTERON WITHIN THE LFD METHOD

The results of the experimental and theoretical studies of the structure and form factors of the deuteron have been presented in the most recent review [41]. In it special attention has been paid to the different theoretical models for investigating the deuteron electromagnetic form factors and nucleon momentum distribution. Among them, the LFD method has been discussed as one of the promising approaches. We start this Section with a brief description of the LFD (e.g. [7–10,42–44]) which is applied to the analyses of relativistic bound systems at high relative momenta. The LFD is a self-consistent method in which the relativistic wave functions are the Fock column components of the state vector defined on an arbitrary light-front (LF) hypersurface given by invariant equation $\omega x = 0$. The four-vector $\omega = (\omega_0, \vec{\omega})$, $\omega^2 = 0$, determines the position of the LF surface. The state vector satisfies a dynamical equation following from rotations of the light front. In LFD the transformations of the reference system and of the light front are independent of each other. The dynamical dependence of the state vector on the LF position is parametrized by the explicit dependence of the wave functions on the four-vector ω. The dependence on ω, however, is not a property of the observable amplitude. The form factors depend on four-momentum transfer squared only and do not depend on ω, though they are related to the ω-dependent wave functions [10]. The relativistic deuteron WF on the LF $\Psi(\vec{q},\vec{n})$ depends on two vector variables: i) the relative momentum $\vec{q}$ and ii) on a unit vector $\vec{n}$ along $\vec{\omega}$. Due to this, the WF is determined by six invariant functions instead of two (S- and D-waves) in the non-relativistic case. Each one of these functions depends on two scalar variables q and $z = cos(\widehat{\vec{q},\vec{n}})$. In LFD these six functions are calculated within the relativistic one-boson-exchange model. The kernel in the dynamical equation for $\Psi(\vec{q},\vec{n})$ has been calculated [10] using Lagrangians of interaction of nucleon with pseudoscalar (π,η)-, scalar (σ,δ)- and vector (ρ,ω) mesons using the parameters of the Bonn model [45]. Thus in the LFD calculations the deuteron structure is determined by the relativistic nucleon-meson dynamics, supposing that the nucleons in the deuteron interact by exchanging relativistic mesons [7], without using potential approximations.

The relations of the covariant LFD method to other relativistic approaches, such as the standard LFD [46], the Bethe-Salpeter formalism [47] and its three-dimensional reductions, the quasi-potential equations [48] and the Gross equation method [49] are given in [9]. For instance, it is shown in [50,9] that after the projection of the Bethe-Salpeter amplitude on the light front, the six components of the LFD deuteron WF are expressed through integrals over the eight components of the deuteron Bethe-Salpeter amplitude. Provided the NN interaction is the same, these approaches incorporate by different methods the same relativistic dynamics. The WF's in LFD are the direct relativistic generalization of the non-relativistic ones in the sense that they are still the probability amplitudes. Therefore they can be used in the relativistic nuclear physics (e.g. [10]). Another advantage of LFD is that due to the explicit relativistic covariance of the method, the form factors do not depend on the system of reference and on the direction of the z-axis. One should emphasize that the LFD WF's have been successfully used also in the hadron physics [51].

As mentioned in the Introduction, the LFD results give a good description of the data [41] for the tensor polarization t_{20} and for the structure function $A(Q^2)$ (up to $Q^2 \simeq 3$ (GeV/c$)^2$). Concerning the structure function $B(Q^2)$ its minimum occurs below the position indicated by the data. The latter is related [7,41] to the insufficient accuracy of the perturbative approach in calculating the components of the LFD wave functions. We would like to emphasize, however, that the LFD method describes very well the charge and quadrupole form factors which are expressed by the structure functions A(Q^2), B(Q^2) and the tensor polarization t_{20}.

In this Section we firstly calculate the nucleon momentum distribution in deuteron $n(q)$ within the LFD using the WF ($\Psi(\vec{q},\vec{n})$) which is normalized generalizing the non-relativistic normalization condition [10]:

$$\frac{1}{3}\frac{m}{(2\pi)^3}\int \Psi^2(\vec{q},\vec{n})\frac{d^3\vec{q}}{\varepsilon(\vec{q})} = \frac{m}{(2\pi)^3}\int F(\vec{q}^2,\vec{n}\cdot\vec{q})\frac{d^3\vec{q}}{\varepsilon(\vec{q})} = 1\,, \tag{1}$$

where F is expressed by the six scalar functions f_{1-6} depending on the scalar variables $\vec{q}^2$ and $\vec{n}\cdot\vec{q}$:

$$F = f_1^2 + f_2^2 + f_3^2 + (3+z^2)f_4^2 + (1-z^2)(f_5^2+f_6^2) + (3z^2-1)f_2f_3 + 4zf_4(f_2+f_3)\,. \tag{2}$$

In (1) $\varepsilon(\vec{q}) = \sqrt{\vec{q}^2+m^2}$, where m is the nucleon mass. As shown in [10], in the non-relativistic limit ($q << m$) the functions f_{3-6} become negligible, $f_{1,2}$ do not depend on z and turn into S- and D-waves ($f_1 \approx u_S$, $f_2 \approx -u_D$) and the WF $\Psi(\vec{q},\vec{n})$ becomes the usual non-relativistic wave function. One of the most important properties of the functions f_{1-6} found in [10] is that for $q \geq 2\div 2.5$ fm^{-1} the component f_5 (being related mainly to π-exchange) exceeds sufficiently the S- and D-waves. This fact is very important in the calculations of $n(q)$ in deuteron as it will be shown below.

In [10] a Legendre expansion of $f_{1-6}(q,z)$ relative to z has been used:

$$f_i(q,z) = \sum_l (2l+1) f_i^l(q) P_l(z) \tag{3}$$

(l=0,2 for i=1,2,3,5 and l=1,3 for i=4,6) with given values of the coefficients $f_i^l(q)$.

We calculate in our work the angle-averaged nucleon momentum distribution in the deuteron defined as:

$$n(q) = C(q)\overline{F(q)}, \tag{4}$$

where

$$C(q) = \frac{m}{(2\pi)^3\varepsilon(q)} \tag{5}$$

and $\overline{F(q)}$ is the angle-averaged function $F(q, z=\cos\theta)$:

$$\overline{F(q)} = \frac{1}{4\pi}\int F(q,\cos\theta)d\Omega. \tag{6}$$

In accordance with Eq. (1) the normalization of $n(q)$ is given by:

$$\int n(\vec{q})d^3\vec{q} = 1\,. \tag{7}$$

The LFD calculations have shown that, as expected, the most important contributions to the total $n(q)$ give terms related to the f_1, f_2 and f_5 functions

$$n(q)\simeq n_1(q) + n_2(q) + n_5(q), \tag{8}$$

where

$$n_1(q) = C(q)\overline{f_1^2(q)}, \quad n_2(q) = C(q)\overline{f_2^2(q)}, \quad n_5(q) = C(q)\overline{(1-z^2)f_5^2(q)}. \tag{9}$$

Here we would like to note that the use of the functions f_1, f_2 and f_5 averaged over $z = cos(\widehat{\vec{q},\vec{n}})$ can be justified by their smooth (almost constant) behaviour as functions of z at different values of q (see Figs. 10 and 11 of [10]). The contributions of n_1, n_2, $n_{12} = n_1 + n_2$ and n_5 are compared in Fig. 1. It can be seen that, while the functions f_1 and f_2 give a good description of the YSD of $n(q)$ for $q < 2$ fm^{-1} (like the S- and D-wave functions in the non-relativistic case), it is impossible to explain the high-momentum components of $n(q)$ at $q > 2$ fm^{-1} without the contribution of the function f_5. We note that the deviation of the total $n(q)$ from the sum $n_{12} = n_1 + n_2$ starts at q around 1.8 fm^{-1}. All this shows the important role of NN interactions which incorporate exchange of relativistic mesons in the case of the deuteron. We emphasize the *consistency of the LFD method obtained in the simultaneous description of both deuteron momentum distribution (made in this work) and of charge form factors* [1]. Here we would like to discuss this point. Considering the LFD results on the nucleon momentum distribution in the deuteron we do not imply that the LFD method and the contribution of the f_5 function are the only way to understand the high-momentum components of $n(q)$. In the following of this Section we will pay attention to the results of other approaches considering, however, this question in close connection to the possibility of simultaneous description of both momentum distribution and form factors. It is known, for instance, that the deuteron wave function related to the Argonne v_{18} potential for the NN interaction [12] gives a realistic description of $n(q)$ in the deuteron [52]. However, as can be seen from Figs. 2 and 4 of Ref. [1], the recent non-relativistic impulse approximation calculations using the Argonne v_{18} potential and even those including meson exchange currents and relativistic corrections do not give a good agreement with the new data of [1] on the tensor polarization t_{20} and the charge form factors G_C and G_Q.

We calculate in the present work also the angle-averaged nucleon momentum distribution in the deuteron using S- and D-wave functions $\Psi_S(q)$ and $\Psi_D(q)$ corresponding to various NN potentials, such as the charge-dependent Bonn potential [53], the Argonne v_{18} [12], the Nijmegen - I ,- II and - Reid 93 [54] and Paris 1980 [55] in the expression:

$$n(q) = \frac{1}{4\pi}[\Psi_S^2(q) + \Psi_D^2(q)] \equiv n_S(q) + n_D(q) \tag{10}$$

with

$$\int n(q) d^3\vec{q} = 1\,. \tag{11}$$

In Fig. 2 the result for $n(q)$ using the charge-dependent Bonn potential [53] is given and compared with the YSD. As can be seen, the D-component of $n(q)$ is important but even its inclusion does not give a very good agreement with the data for $q \geq 2$ fm^{-1}. In the next Fig. 3 we present the LFD result for $n(q)$ compared with the calculations using the WF's corresponding to Nijmegen-I,-II, -Reid 93, Argonne v$_{18}$ and Paris 1980 NN potentials and with the y-scaling data. We would like to note that: i) the results of the calculations using the NN potentials, such as Nijmegen-II, -Reid 93, Argonne v$_{18}$ and Paris 1980 (shown in Fig. 3) are in better agreement with the YSD than those using the charge-dependent Bonn potential (Fig. 2). This might be related to the fact that these potentials describe NN phase shifts up to larger energies (e.g. the Nijmegen-II potential gives reasonable pp phase shifts up to 1.2 GeV, while the charge-dependent one-boson exchange Bonn potential fits the phase-shift data below 350 MeV); ii) It can be seen from Fig. 3 that there are small differences between the curves corresponding to different NN potentials for $q \leq 3$ fm^{-1} (which give a good description of the YSD and almost coincide with the LFD result) and larger ones for $q > 3$ fm^{-1}. Large differences take place, however, between all of them and the LFD result for $q > 3$ fm^{-1}. An important conclusion of this fact is that data at higher momentum transfers are needed (and probably a more refined analysis of the currents used for the coupling of the electron with the nucleons) in order to distinguish the properties of the covariant LFD method from the potential approaches. The momentum region of q just larger than 3 fm^{-1} will be decisive in this sense. The main advantage of the LFD method is, however, as mentioned already, that it describes simultaneously the deuteron charge form factors as well, which is not the case with e.g. the Argonne v$_{18}$ NN potential method (see Fig. 4 in [1]).

III. NUCLEON MOMENTUM DISTRIBUTIONS IN ^{4}He, ^{12}C AND ^{56}Fe

As mentioned in the Introduction, realistic many-body calculations (e.g. [20–40,14,15]) have shown the existence of high-momentum components in the nucleon momentum distributions for studied nuclei at $q \geq 2$ fm^{-1}, due to presence of short-range and tensor correlations. This conclusion agrees well with the y-scaling data [16–19]. Secondly, it has been shown that all nuclear momentum distributions $n_A(q)$

for (A, Z)-nuclei $(A > 2)$ at these high momenta are simply rescaled versions of the nucleon momentum distribution in the deuteron $n(q)$ [56]:

$$n_A(q) \cong \alpha_A n(q), \tag{12}$$

where α_A is a constant.

Since the magnitude of the high-momentum tail of $n_A(q)$ is proportional to the mass number, this effect is associated with the nuclear interior rather than with the nuclear surface. In the present paper we develop a model to calculate $n_A(q)$ for nuclei with $A > 2$ from that of the deuteron. The method has similarities to that suggested in [57] on the basis of ^{4}He. However, in the present work we incorporate the analysis performed in Sect. II for the deuteron as the simplest two-nucleon bound system to the consideration of $n_A(q)$ for heavier nuclei, namely because the high-momentum components are related to the specific features of the two-nucleon interaction at short distance (around the repulsive core). The latter determine the corresponding behaviour of the nucleons in the central part of the nucleus, where the density is higher. There the two nucleons could be closer to one another and the short-range correlations could be operative. In this sense, we consider the present method as a next step and improvement on that of [57].

In this Section we suggest a practical method to calculate the nucleon momentum distribution for the general case of (A, Z)-nuclei $(A > 2)$, while as we mentioned already, the correlation methods consider only particular nuclei (e.g. ^{3,4}He, ^{12}C, ^{16}O, ^{40}Ca and nuclear matter) and due to their complexity the applications to other nuclei is often a very difficult task.

We use the natural orbital representation (NOR) [58,14,15] of the one-body density matrix. In our case we consider its diagonal elements in the momentum space, which represent the nucleon momentum distribution $n_A(q)$. The NOR allows us to use the transparency of the single-particle picture even being beyond the mean-field approximation and to account for the correlation effects in a proper way. Using the common theoretical ground of NOR, the method makes it possible to combine the mean-field predictions for $n_A(q)$ (which are expected to be realistic at $q < 2$ fm^{-1}) with that part of the momentum distribution which includes correlation and relativistic effects.

In the natural orbital representation the momentum distribution in a nucleus with A nucleons can be written in the form:

$$n_A(q) = N_A[n_A^h(q) + n_A^p(q)], \tag{13}$$

where N_A is the normalization constant and

$$n_A^h(q) = \frac{1}{A}\sum_{nlj}^{F.L.} 2(2j+1)\lambda_{nlj} C(q) |R_{nlj}(q)|^2 \tag{14}$$

$$n_A^p(q) = \frac{1}{A}\sum_{F.L.}^{\infty} 2(2j+1)\lambda_{nlj} C(q) |R_{nlj}(q)|^2 \tag{15}$$

are the hole- and particle-state contributions, respectively. In (14) and (15) F.L. denotes the Fermi level, $C(q)$ is given by (5), λ_{nlj} are the natural occupation numbers ($0 \leq \lambda_{nlj} \leq 1$) for a state with quantum numbers nlj and $R_{nlj}(q)$ are the natural orbitals. We call hole-state natural orbitals those natural orbitals for which the numbers λ_{nlj} are significantly larger than the remaining ones, called particle-state natural orbitals [59]. As shown in [39], the high-momentum components of the total $n_A(q)$ caused by short-range correlations are almost completely determined by the contributions of the particle-state natural orbitals. This fact, together with the approximate equality of the high-momentum tails of $n(q)/A$ for all nuclei allows us to make the main assumption of the method that the particle-state contributions to $n_A(q)$ are almost equal for all nuclei. The deuteron $n(q)$ from (8) can be written in a form similar to (13):

$$n(q) = N_d[n_d^h(q) + n_d^p(q)] \tag{16}$$

with

$$n_d^h(q) = \frac{1}{2}[n_1(q) + n_2(q)], \tag{17}$$

$$n_d^p(q) = \frac{1}{2} n_5(q), \tag{18}$$

and $N_d = 2$. The assumed equality of the particle-state contributions for all nuclei implies the equality of the particle-state contribution $n_A^p(q)$ for (A, Z)-nuclei from (15) with that to the deuteron momentum distribution $n_d^p(q)$ from (18)

$$n_A^p(q) \simeq n_d^p(q). \tag{19}$$

The right-hand side of (19) can be taken from different sources. This could be the YSD or results of calculations within given theoretical correlation models. Having the results from Sect. II we take $n_d^p(q)$ to be related to $n_5(q)$ (18) because within the LFD namely this function is responsible for the high-momentum tail of $n(q)$ for deuteron:

$$n_A^p(q) \cong \frac{1}{2} n_5(q)\,. \tag{20}$$

Then the resulting momentum distribution for (A, Z)-nucleus normalized to unity has the form:

$$n_A(q) = N_A[\sum_{nlj}^{F.L.} 2(2j+1)\lambda_{nlj} C(q) |R_{nlj}(q)|^2 + \frac{A}{2} n_5(q)] \,, \tag{21}$$

where

$$N_A = \{4\pi \int dq {\cdot} q^2 [\sum_{nlj}^{F.L.} 2(2j+1)\lambda_{nlj} C(q) |R_{nlj}(q)|^2 + \frac{A}{2} n_5(q)]\}^{-1} \,. \tag{22}$$

It is known from [39] that the hole-state natural orbitals are almost unaffected by the short-range correlations and, therefore, the functions $R_{nlj}(q)$ in (21) and (22) can be replaced by single-particle wave functions from the mean-field approximation (shell-model or Hartree-Fock WF). In our calculations we use Woods-Saxon s.p. wave functions for protons and neutrons. The hole-state occupation numbers λ_{nlj} are close to unity and we set them equal to unity with good approximation. These properties lead to a similarity of our model to that suggested for calculations of the spectral function [60].

The calculations of $n_A(q)$ for ^{4}He,^{12}C and ^{56}Fe are given in Figs. 4-6 and are compared with the y-scaling data from [18]. We note that, as expected from (12) the value of α_A must be almost constant. In our case $\alpha_A = N_A \cdot A/2$ and its numerical values are 8.335, 8.352 and 8.372 for ^{4}He, ^{12}C and ^{56}Fe, respectively.

The dashed line in Figs. 4-6 gives the calculated normalized hole-state contribution (the mean-field component) to $n_A(q)$ only, i.e. without the contribution of $n_5(q)$ in Eq. (21). The comparison between the total $n_A(q)$, its hole-state contribution and the y-scaling data clearly shows the role of $n_5(q)$ contribution. It can be seen that the difference between the results with $n_5(q)$ and without it starts for all three nuclei at $q \simeq 1.5$ fm^{-1} and increase rapidly at $q > 1.5$ fm^{-1}. This shows the role of the high-momentum components of the deuteron momentum distribution n_5 which can be considered as an "ingredient" of the high-momentum components of the momentum distribution of (A, Z)-nucleus. In our opinion, the related function f_5 of the LFD method incorporates the main part of the short-range features of the NN interactions which determine the correlation effects seen in $n_A(q)$ when calculated within the non-relativistic correlation methods.

The good agreement of the results on $n_A(q)$ with the data for the three nuclei achieved, including also the region of the high momenta, proves the assumption that the nucleon momentum distribution in nuclei can be extracted on the basis of the realistically described properties of the deuteron as the smallest bound system of two nucleons.

IV. CONCLUSIONS

The results of the present work can be summarized as follows:

(i) The light-front dynamics method is applied to calculate the nucleon momentum distribution in the deuteron. A very good description of the y-scaling data is obtained. It is shown that, while the functions f_1 and f_2 describe well the YSD of $n(q)$ for $q < 2$ fm^{-1}, it is impossible to explain the high-momentum components of $n(q)$ at $q > 2$ fm^{-1} without the contribution of the function f_5. Thus, this study gives a positive answer to the question about the possibilities of the LFD method *to describe simultaneously* both deuteron momentum distribution and charge form factors (the good agreement with the latter as well as with the data for the tensor polarization t_{20} and for the structure function $A(Q^2)$ up to $Q^2 \simeq 3$ (GeV/c)^2 was shown in [1,41]).

(ii) The nucleon momentum distribution in deuteron was calculated also in this work using the S- and D-wave functions corresponding to various NN potentials (charge-dependent Bonn, Paris 1980, Nijmegen-I and -II, -Reid 93, Argonne v$_{18}$). We show that the results using these potentials explain very well (with the exception of the charge-dependent Bonn potential) all the available data for $n(q)$ up to $q \simeq 3$ fm^{-1} exactly like the LFD method. However, as shown in [1], the recent non-relativistic impulse approximation calculations (e.g. with Argonne v$_{18}$ potential) and even those including meson exchange currents and relativistic corrections do not describe well the new data [1] on the tensor polarization t_{20} and the charge form factors G_C and G_Q. This is the main difference between the results of the LFD method and of the calculations using WF's corresponding to NN potentials for the important deutron characteristics considered. Secondly, we should mention also that for $q > 3$ fm^{-1} the LFD results for $n(q)$ deviate strongly from those of the calculations using NN potentials. Thus data at higher q are needed in order to distinguish the abilities of the LFD from those of the potential methods. Here we would like to mention also other relativistic methods such as the method in [11] (using a three-dimensional reduction of the Bethe- Salpeter equation) and the method in [61] (based on the Gross equation [49]) which could give a simultaneous description of both deuteron form factors and momentum distribution.

(iii) A correlation method for calculating the nucleon momentum distribution in nuclei with $A > 2$ $n_A(q)$ is proposed. The method uses the natural orbital representation of the one-body density matrix and combines the mean-field component of $n_A(q)$ with the correlated high-momentum components taken from the deuteron momentum distribution. The method is based on the well-known results of realistic many-body calculations which have shown that, due to the short-range and tensor NN correlations, all nuclear momentum distributions $n_A(q)$ at high momenta ($q > 2$ fm^{-1}) are rescaled versions of the nucleon momentum distribution in the deuteron $n(q)$. In the present work we incorporate in the method the LFD results for $n(q)$. The role of the wave function f_5 is clearly shown by the comparison of the calculations of $n_A(q)$ using the hole-state (mean-field) contribution without and with an inclusion of the $n_5(f_5)$ contribution. In our opinion, the LFD function f_5 incorporates the main part of the short-range features of the NN interactions which can be seen in calculations of $n_A(q)$ within non-relativistic correlation methods. The suggested method gives an easy practical way for calculations of $n_A(q)$ for any nucleus because only hole-state wave functions and occupation probabilities enter its main relationships (Eqs.(21) and (22)). The method gives a good description of the y-scaling data for $n_A(q)$ in ^{4}He, ^{12}C and ^{56}Fe including the high-momentum region, showing a clear difference from the mean-field predictions for $q > 1.5$ fm^{-1}.

V. ACKNOWLEDGMENTS

One of the authors (A.N.A.) thanks Prof. V.A. Karmanov and Prof. J. Carbonell for the helpful discussions. He is also grateful to the Royal Society in London and the Bulgarian Academy of Sciences for support during his visit to the University of Oxford. The work was partly supported by the Bulgarian National Science Foundation (Contracts No.$\Phi - 809$ and $\Phi - 905$).

---

[1] D. Abott et al., Jefferson Lab. t$_{20}$ Collaboration, Phys. Rev. Lett. **84**, 5053 (2000).

[2] D. Abott et al., Jefferson Lab. t$_{20}$ Collaboration, Eur. Phys. J. **A7**, 421 (2000).

[3] D. Abott et al., Jefferson Lab. t$_{20}$ Collaboration, Phys. Rev. Lett. **82**, 1379 (1999).

[4] L.C. Alexa et al., Jefferson Lab. Hall A Collaboration, Phys. Rev. Lett. **82**, 1374 (1999).

[5] C. Furget et al., Acta Phys. Pol. **B29**, 3301 (1998).

[6] E. Beise, Few-Body Systems Suppl. **10**, 315 (1999).

[7] J. Carbonell and V.A. Karmanov, Eur. Phys. J. A **6**, 9 (1999).

[8] V.A. Karmanov, Fiz. Elem. Chastits At. Yadra **19**, 525 (1988) (Sov. J. Part. Nucl. **19**, 228 (1988)).

[9] J. Carbonell, B. Desplanques, V.A. Karmanov, and J.-F. Mathiot, Phys. Rep. **300**, 215 (1998).

[10] J. Carbonell and V.A. Karmanov, Nucl. Phys. **A581**, 625 (1995).

[11] D.R. Phillips, S.J. Wallace, and N.K. Devine, nucl-th /9906086 (1999); Phys. Rev. C **58**, 2261 (1998); D.R. Phillips and S.J. Wallace, Few-Body Systems **24**, 175 (1998).

[12] R.B. Wiringa, V.G.J. Stoks, and R. Schiavilla, Phys. Rev. C **51**, 38 (1995).

[13] M. Jaminon, C. Mahaux, and H. Ngô, Phys. Lett. **158B**, 103 (1985).

[14] A.N. Antonov, P.E. Hodgson, and I.Zh. Petkov, *Nucleon Momentum and Density Distributions in Nuclei* (Clarendon, Oxford, 1988).

[15] A.N. Antonov, P.E. Hodgson, and I.Zh. Petkov, *Nucleon Correlations in Nuclei* (Springer-Verlag, Berlin, 1993).

[16] D.B. Day, J.S. McCarthy, T.W. Donnelly, and I. Sick, Annu.Rev.Nucl.Part.Sci. **40**, 357 (1990).

[17] C. Ciofi degli Atti, E. Pace, and G. Salmè, Phys. Rev. C **36**, 1208 (1987).

[18] C. Ciofi degli Atti, E. Pace, and G. Salmè, Phys. Rev. C **43**, 1155 (1991); Preprint INFN-ISS 90/8, Roma (1990).

[19] C. Ciofi degli Atti and S. Simula, Phys. Rev. C **53**, 1689 (1996).

[20] R.D. Amado, Phys. Rev. C **14**, 1264 (1976).

[21] J.G. Zabolitzky and W. Ey, Phys. Lett. **76B**, 527 (1978).

[22] J.W. van Orden, W. Truex, aand M.K. Banerjee, Phys. Rev. C **21**, 2628 (1980).

[23] O. Bohigas and S. Stringari, Phys. Lett. **95B**, 9 (1980).

[24] A.N. Antonov, V.A. Nikolaev, and I.Zh. Petkov, Z. Phys. **A297**, 257 (1980).

[25] F. Dellagiacoma, G. Orlandini, and M. Traini, Nucl. Phys. **A393**, 95 (1983).

[26] C. Ciofi degli Atti, E. Pace, and G. Salmè, Phys. Lett. **141B**, 14 (1984).

[27] S. Fantoni and V.R. Pandharipande, Nucl. Phys. **A427**, 473 (1984).

[28] Y. Akaishi, Nucl. Phys. **A416**, 409c (1984).

[29] M.F. Flynn, J.W. Clark, R.M. Panoff, O. Bohigas, and S. Stringari, Nucl. Phys. **A427**, 253 (1984).

[30] M. Traini and G. Orlandini, Z. Phys. **A321**, 479 (1985).

[31] O. Benhar, C. Ciofi degli Atti, S. Liuti, and G. Salmè, Phys. Lett. **177B**, 135 (1986).

[32] R. Schiavilla, V.R. Pandharipande, and R.B. Wiringa, Nucl. Phys. **A449**, 219 (1986).

[33] M. Jaminon, C. Mahaux, and H. Ngô, Nucl. Phys. **A452**, 445 (1986).

[34] H. Morita, Y. Akaishi, and H. Tanaka, Prog. Theor. Phys. **79**, 863 (1988).

[35] S. Stringari, M. Traini, and O. Bohigas, Nucl. Phys. **A516**, 33 (1990).

[36] S.C. Pieper, R.B. Wiringa, and V.R. Pandharipande, Phys. Rev. Lett. **64**, 364 (1990); Phys. Rev. C **46**, 1741 (1992).

[37] M. Baldo, I. Bombaci, G. Giansiracusa, U. Lombardo, C. Mahaux, and R. Sartor, Phys. Rev. C **41**, 1748 (1990).

[38] A.N. Antonov, P.E. Hodgson, and I.Zh. Petkov, Nuovo Cimento **A97**, 117 (1987); A.N. Antonov, I.S. Bonev, Chr.V. Christov, and I.Zh. Petkov, Nuovo Cimento **A100**, 779 (1988); A.N. Antonov, M.V. Stoitsov, L.P. Marinova, M.E. Grypeos, G.A. Lalazissis, and K.N. Ypsilantis, Phys. Rev. C **50**, 1936 (1994).

[39] M.V. Stoitsov, A.N. Antonov, and S.S. Dimitrova, Phys. Rev. C **47**, R455 (1993); Phys. Rev. C **48**, 74 (1993).

[40] H. Müther, A. Polls, and W.H. Dickhoff, Phys. Rev. C **51**, 3040 (1995).

[41] M. Garçon and J.W. Van Orden, nucl-th/0102049 (2001).

[42] V.A. Karmanov, Nucl. Phys. **A362**, 331 (1981).

[43] V.A. Karmanov and A.V. Smirnov, Nucl. Phys. **A546**, 691 (1992).

[44] V.A. Karmanov and A.V. Smirnov, Nucl. Phys. **A575**, 520 (1994).

[45] R. Machleidt, K. Holinde, and Ch. Elster, Phys. Rep. **149**, 1 (1987).

[46] P.A.M. Dirac, Rev. Mod. Phys. **21**, 392 (1949).

[47] E.E. Salpeter and H.A. Bethe, Phys. Rev. **84**, 1232 (1951).

[48] A.A. Logunov and A.N. Tavkhelidze, Nuovo Cimento **29**, 370 (1963); R. Blankenbecler and R. Sugar, Phys. Rev. **142**, 1951 (1966).

[49] F. Gross, Phys. Rev. **186**, 1448 (1969); Phys. Rev. D **10**, 223 (1974); Phys. Rev. C **26**, 2203 (1982).

[50] S. Bondarenko, V.V. Burov, M. Beyer, and S.M. Dorkin, Few-Body Systems **26**, 185 (1999); nucl-th/9811022.

[51] S.J. Brodsky, H.-C. Pauli, and S.S. Pinsky, Phys. Rep. **301**, 299 (1998).

[52] J.L. Forest, V.R. Pandharipande, S.C. Pieper, R.B. Wiringa, R. Schiavilla, and A. Arriaga, Phys. Rev. C **54**, 646 (1996).

[53] R. Machleidt, Phys. Rev. C **63**, 024001 (2001).

[54] V.G.J. Stoks, R.A.M. Klomp, C.P.F. Terheggen, and J.J. de Swart, Phys. Rev. C **49**, 2950 (1994).

[55] M. Lacombe, B. Loiseau, J.M. Richard, R. Vinh Mau, J. Côté, P. Pirès, and R. de Tourreil, Phys. Rev. C **21**, 861 (1980).

[56] D. Faralli, C. Ciofi degli Atti, and G.B. West, *Proceedings of 2nd Int. Conf. on Perspectives in Hadronic Physics*, ICTP, Trieste, Italy , 10-14 May 1999, edited by S. Boffi, C. Ciofi degli Atti, and M.M. Giannini, (World Scientific, Singapore, 2000), p.75.

[57] M.K. Gaidarov, A.N. Antonov, G.S. Anagnostatos, S.E. Massen, M.V. Stoitsov, and P.E. Hodgson, Phys. Rev. C **52**, 3026 (1995).

[58] P.-O. Löwdin, Phys. Rev. **97**, 1474 (1955).

[59] D.S. Lewart, V.R. Pandharipande, and S.C. Pieper, Phys. Rev. B **37**, 4950 (1988).

[60] O. Benhar, A. Fabrocini, S. Fantoni, and I. Sick, Nucl. Phys. **A579**, 493 (1994).

[61] J.W. Van Orden, N. Devine, and F. Gross, Phys. Rev. Lett. **75**, 4369 (1995); Few Body Systems Suppl. **9**, 415 (1995); J.W. Van Orden, Czech. J. Phys. **45**, 181 (1995).

FIG. 1. The nucleon momentum distribution in deuteron. The contributions of n_1, n_2, $n_{12} = n_1 + n_2$ and n_5 are presented. The y-scaling data are from [18]. The normalization is: $\int n(q) d^3\vec{q} = 1$.

FIG. 2. The nucleon momentum distribution in deuteron (solid line) calculated using Eqs. (10) and (11) with S- and D-wave functions corresponding to the charge-dependent Bonn potential [53]. S- and D-contributions are given by dashed and dotted line, respectively. The y-scaling data are from [18].

FIG. 3. The nucleon momentum distribution in deuteron calculated with the LFD (solid line) in comparison with the results presented by numerated arrows, as follows: 1-Argonne v_{18}, 2-Nijmegen Reid 93, 3-Nijmegen I, 4-Nijmegen II, 5-Paris 1980 NN potentials and with the y-scaling data [18].

FIG. 4. The nucleon momentum distribution in ^{4}He calculated using Eqs. (21) and (22) (solid line). The dotted line represents the hole-state contribution only. The y-scaling data are from [18]. The normalization is: $\int n_A(q) d^3\vec{q} = 1$.

FIG. 5. The same as in Fig.4 for ^{12}C.

FIG. 6. The same as in Fig.4 for ^{56}Fe.

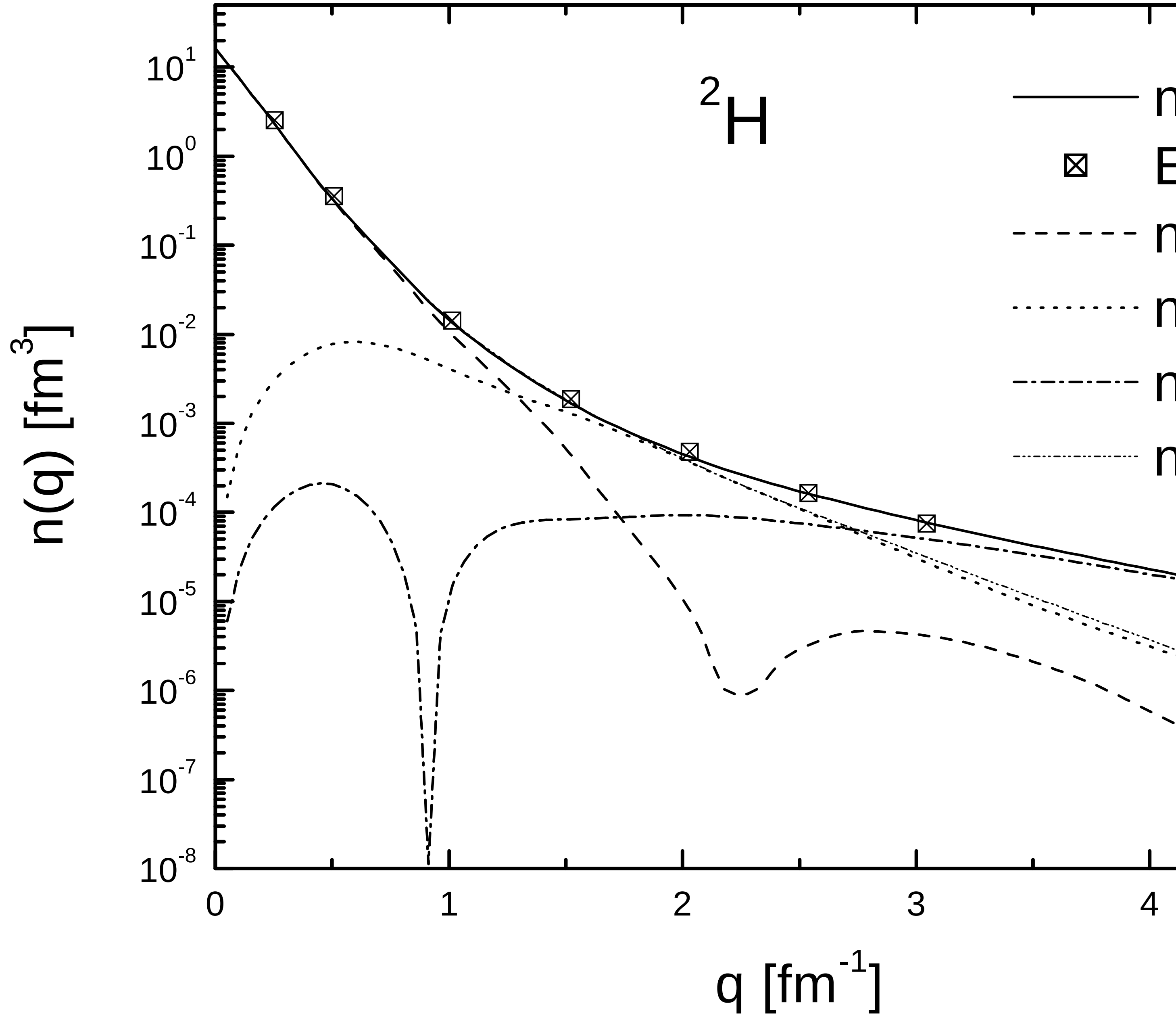

²H
n
E
n
n
n
n
n(q) [fm³]
q [fm⁻¹]
10¹
10⁰
10⁻¹
10⁻²
10⁻³
10⁻⁴
10⁻⁵
10⁻⁶
10⁻⁷
10⁻⁸
0
1
2
3
4

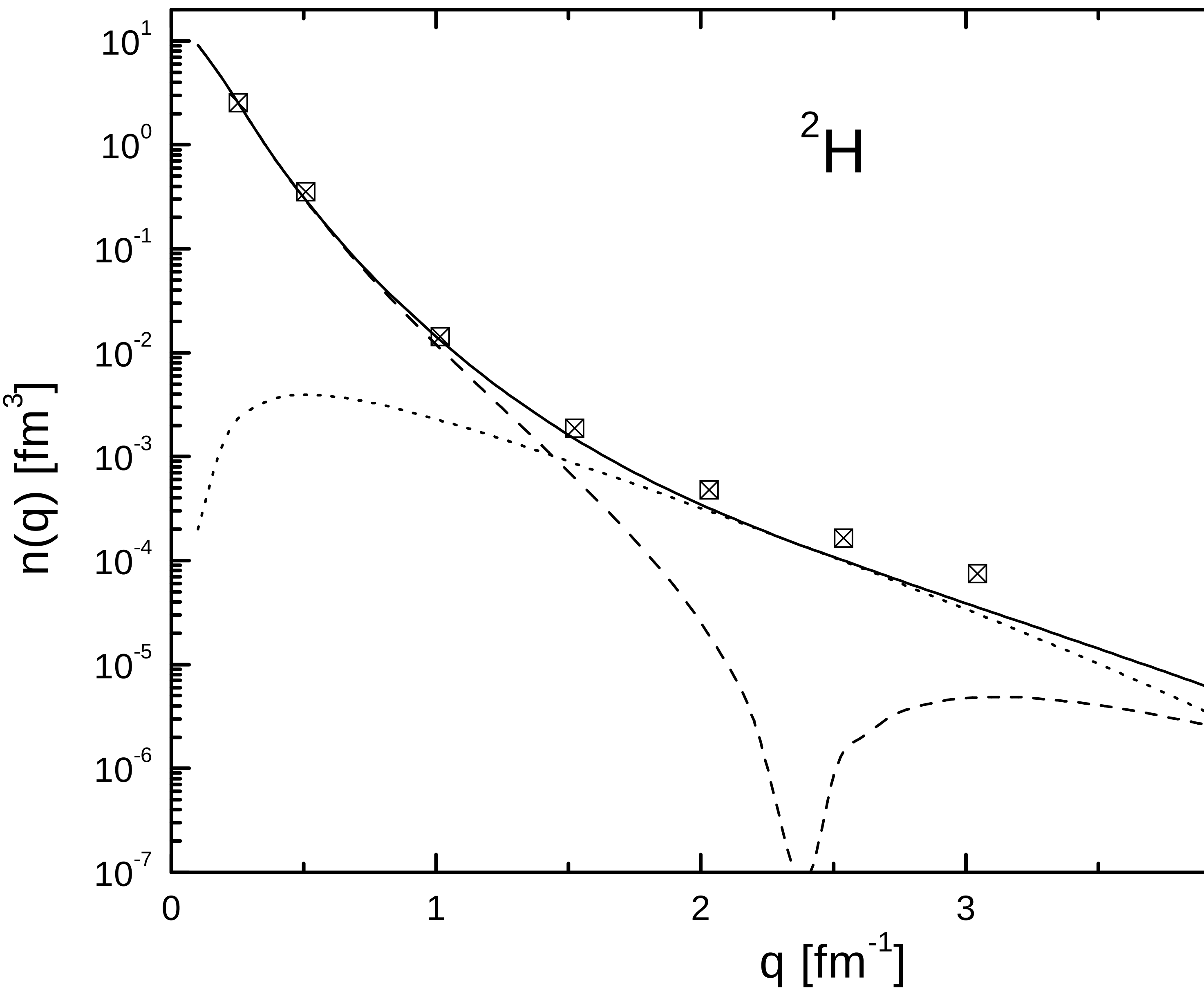

^{2}H
n(q) [fm^3]
q [fm^{-1}]
10^{1}
10^{0}
10^{-1}
10^{-2}
10^{-3}
10^{-4}
10^{-5}
10^{-6}
10^{-7}
0
1
2
3

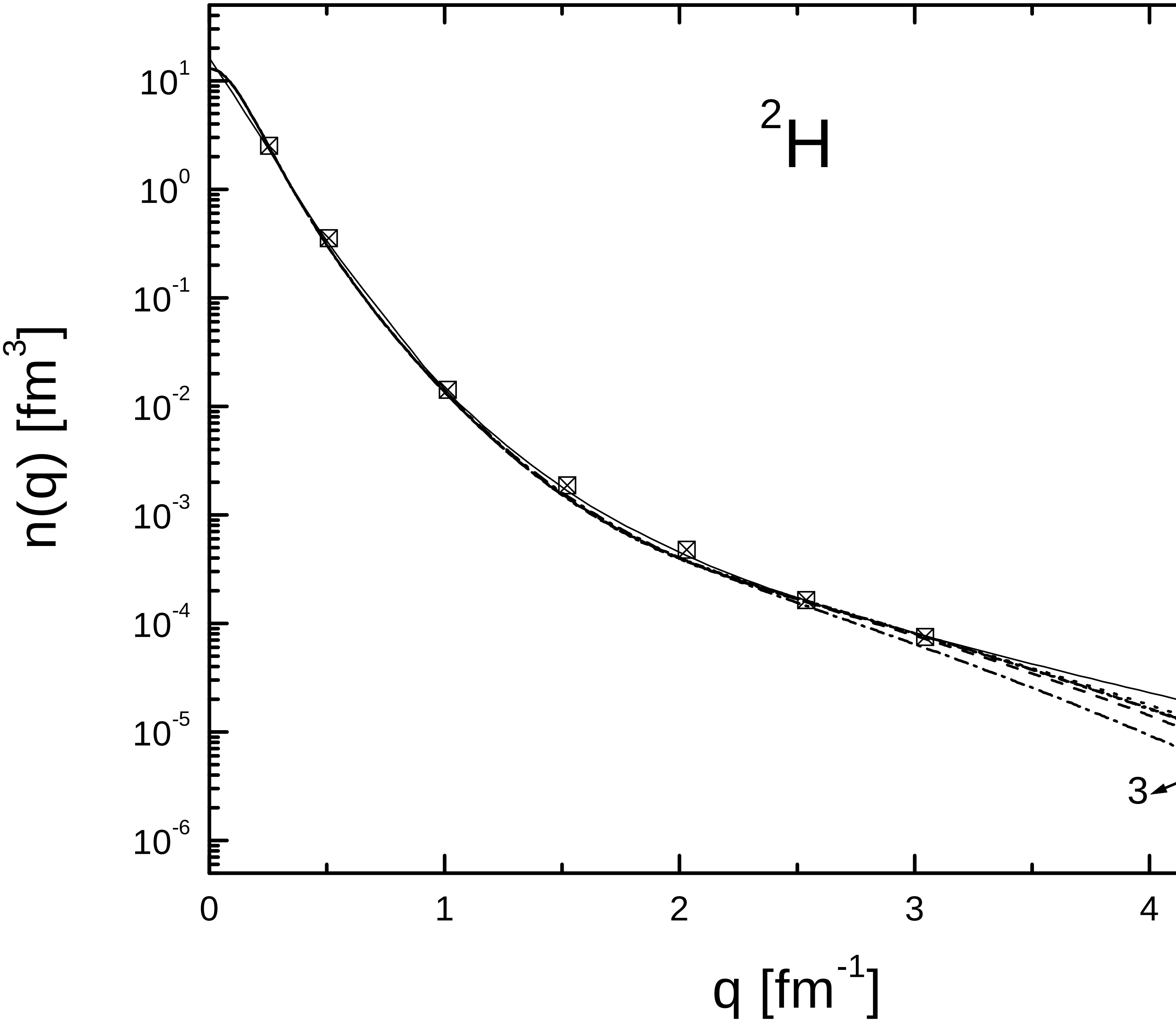
^{2}H
n(q) [fm^3]
q [fm^{-1}]
10^1
10^0
10^{-1}
10^{-2}
10^{-3}
10^{-4}
10^{-5}
10^{-6}
0
1
2
3
4
3

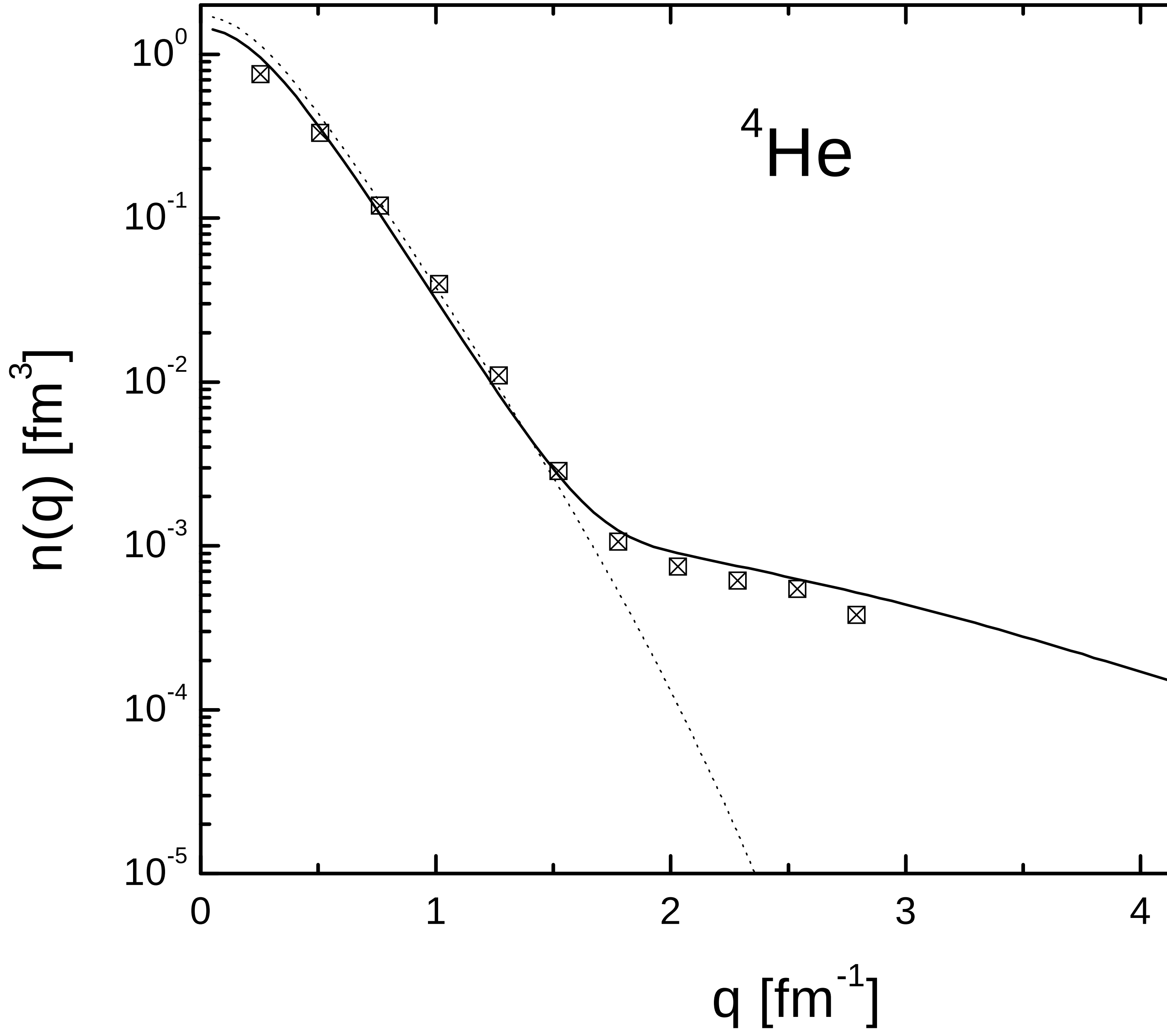

^{4}He
n(q) [fm^3]
q [fm^{-1}]
10^0
10^{-1}
10^{-2}
10^{-3}
10^{-4}
10^{-5}
0
1
2
3
4

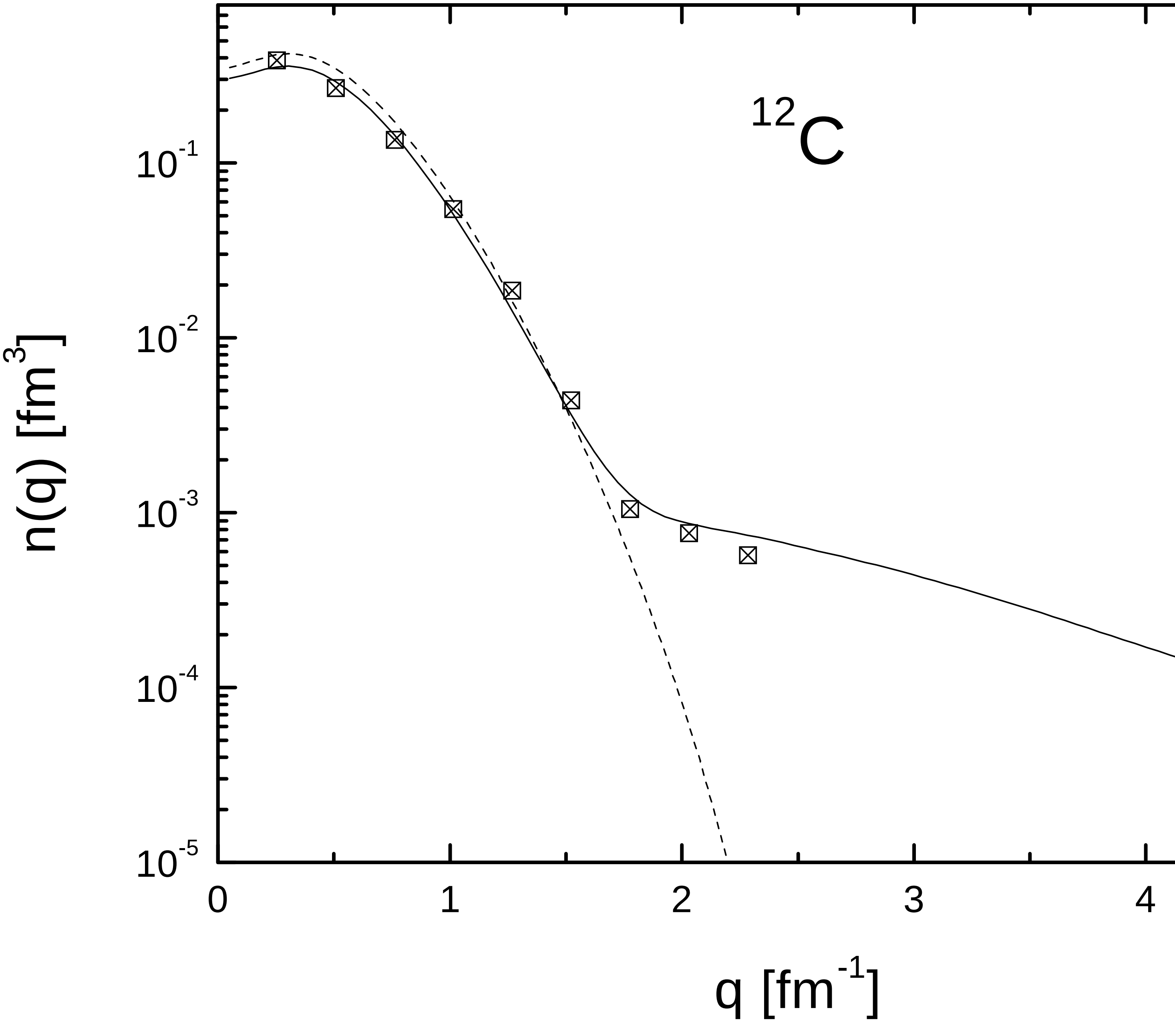

^{12}C
n(q) [fm^3]
q [fm^{-1}]
10^{-1}
10^{-2}
10^{-3}
10^{-4}
10^{-5}
0
1
2
3
4

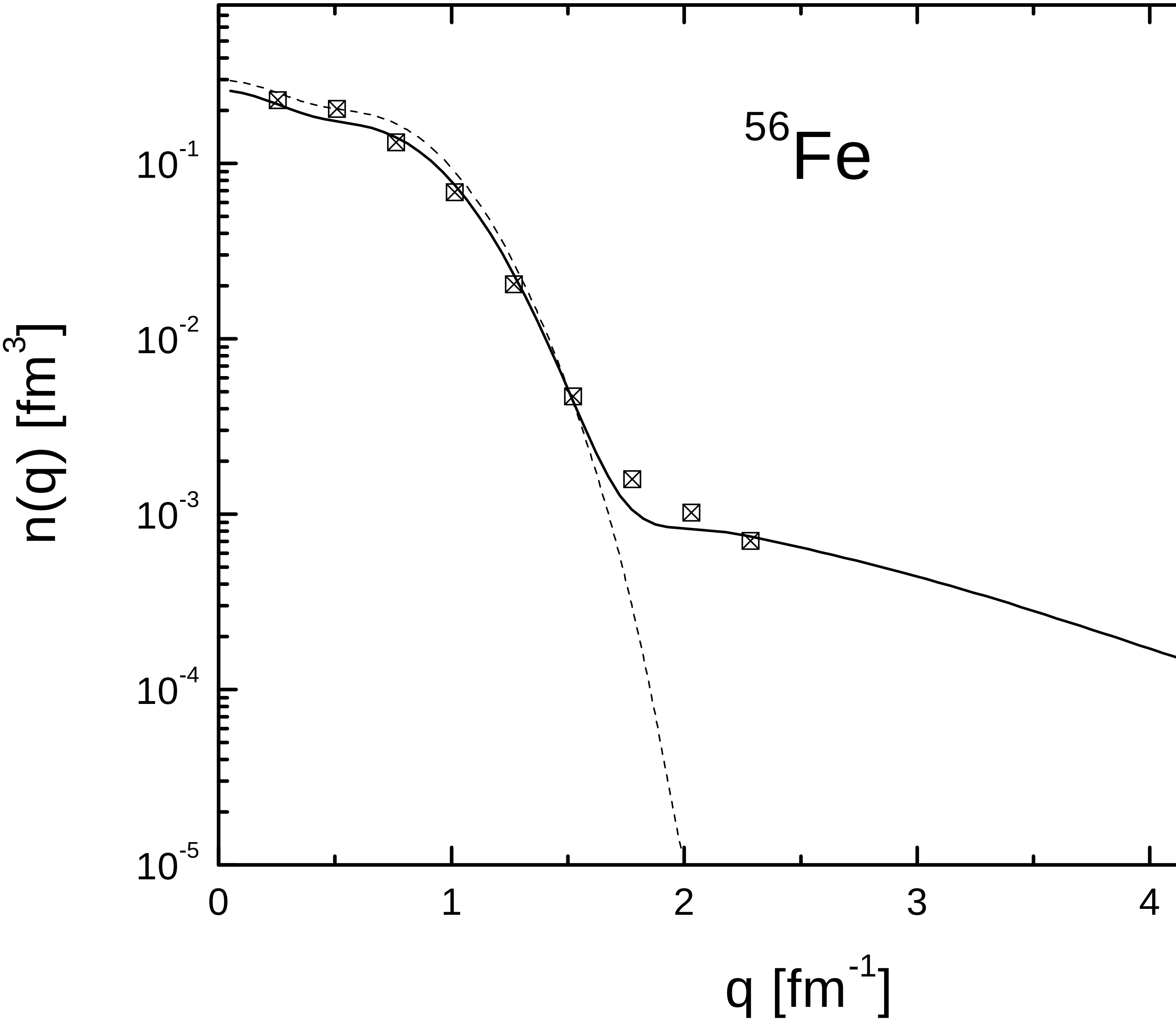
^{56}Fe
n(q) [fm^3]
10^{-1}
10^{-2}
10^{-3}
10^{-4}
10^{-5}
0
1
2
3
4
q [fm^{-1}]